A Nomogram Combining a Four-Gene Biomarker and Clinical Factors for Predicting Survival of Melanoma

Chuan Zhang[1], Dan Dang[2], Yuqian Wang[3] and Xianling Cong[4]*

[1] Department of Pediatric Surgery, The First Hospital of Jilin University, Changchun, China, [2] Department of Neonatology, The First Hospital of Jilin University, Changchun, China, [3] Scientific Research Center, China-Japan Union Hospital of Jilin University, Changchun, China, [4] Department of Dermatology, China-Japan Union Hospital of Jilin University, Changchun, China

Background: Currently there is no effective prognostic indicator for melanoma, the deadliest skin cancer. Thus, we aimed to develop and validate a nomogram predictive model for predicting survival of melanoma.

Methods: Four hundred forty-nine melanoma cases with RNA sequencing (RNA-seq) data from TCGA were randomly divided into the training set I (n = 224) and validation set I (n = 225), 210 melanoma cases with RNA-seq data from Lund cohort of Lund University (available in GSE65904) were used as an external test set. The prognostic gene biomarker was developed and validated based on the above three sets. The developed gene biomarker combined with clinical characteristics was used as variables to develop and validate a nomogram predictive model based on 379 patients with complete clinical data from TCGA (Among 470 cases, 91 cases with missing clinical data were excluded from the study), which were randomly divided into the training set II (n = 189) and validation set II (n = 190). Area under the curve (AUC), concordance index (C-index), calibration curve, and Kaplan-Meier estimate were used to assess predictive performance of the nomogram model.

Results: Four genes, i.e., *CLEC7A*, *CLEC10A*, *HAPLN3*, and *HCP5* comprise an immune-related prognostic biomarker. The predictive performance of the biomarker was validated using tROC and log-rank test in the training set I (n = 224, 5-year AUC of 0.683), validation set I (n = 225, 5-year AUC of 0.644), and test set I (n = 210, 5-year AUC of 0.645). The biomarker was also significantly associated with improved survival in the training set (P < 0.01), validation set (P < 0.05), and test set (P < 0.001), respectively. In addition, a nomogram combing the four-gene biomarker and six clinical factors for predicting survival in melanoma was developed in the training set II (n = 189), and validated in the validation set II (n = 190), with a concordance index of 0.736 ± 0.041 and an AUC of 0.832 ± 0.071.

Conclusion: We developed and validated a nomogram predictive model combining a four-gene biomarker and six clinical factors for melanoma patients, which could facilitate risk stratification and treatment planning.

Keywords: prognostic biomarker, nomogram, microenvironment, melanoma, immune genes

INTRODUCTION

Cutaneous melanoma is the deadliest type of skin cancer (1, 2), and its morbidity has been on the rise annually, especially in the Caucasian population (3, 4). As melanoma is generally recognized as a highly heterogeneous cancer (5) and immunotherapy remains the preferred treatment for advanced melanoma (6), immune-related biomarkers have been exploited as prognostic signatures of melanoma (7–10). However, the current existing immune-related prognostic biomarkers have their limitations. For instance, some biomarkers contain a relatively large number of genes that reduces their potential applicability to some extent (7, 8), while for others, there is a lack of detailed information regarding the potential mechanism and clinical relevance (8, 9). Therefore, the identification of a comparatively reliable and applicable prognostic biomarker for melanoma in order to guide clinical decision-making is essential.

Considering the advancements in gene sequencing technology, a set of gene databases, such as The Cancer Genome Atlas (TCGA) (11, 12) and Gene Expression Omnibus (GEO) have emerged as popular guide sources. A series of bioinformatics tools, including weighted gene co-expression network analysis (WGCNA) (13), cell-type identification by estimating relative subsets of RNA transcripts (CYBERSORT) (14), gene set enrichment analysis (GSEA) (15, 16), and least absolute shrinkage and selection operator (LASSO), have been used to process such big data. The strategy of using a combination of these databases and bioinformatics tools in scientific practice is supported by the reliability of such approaches (17–21).

To identify an immune-related prognostic biomarker and develop a new nomogram predictive model for melanoma patients, we analyzed the RNA sequencing (RNAseq) data and the corresponding clinical data from TCGA and GEO databases using bioinformatic tools. The findings would show useful prognostic factors and a nomogram for predicting survival in melanoma patients. Researchers, clinicians, and patients would handily forecast the survival probability for each individual patient using this nomogram.

MATERIALS AND METHODS

Data Acquisition

Four hundred seventy-two melanoma cases with RNA sequencing data were download from TCGA, and 449 of them with complete survival data were randomly divided into the training set I (n = 224) and validation set I (n = 225) (**Table S1**). Two hundred fourteen melanoma cases with RNA sequencing data and survival data were obtained from Lund cohort of Lund University (available in GSE65904) (22, 23) and 210 of them with complete survival data were utilized as an external test set (**Table S1**). The above three sets were used to identify and validate a prognostic gene biomarker.

Four hundred seventy melanoma cases with clinical data were obtained from TCGA and 91 cases with missing clinical data were excluded from the study. Of them, 379 met our inclusion criterion that they do not contain any missing data for selected variables including age, gender, overall survival time, survival status, and clinical stage. The 379 cases were subsequently randomly assigned to the training set II (n = 189) and validation set II (n = 190) (**Table S2**), which were used to develop and validate a nomogram predictive model. In developing the nomogram, the four-gene biomarker and clinical characteristics were used as variables.

Immune, stromal, and estimate scores of each patient were available from the ESTIMATE database (**Table S2**) (24). A total of 5,559 human immune genes were downloaded from the InnateDB database (**Table S2**) (25).

WGCNA

WGCNA, a reliable and approved bioinformatics method, was employed to identify immune-related modules. We first removed outlier genes and genes expressed at extremely low levels from the data. Construction of a weighted gene network involves the choice of the soft thresholding power β to which co-expression similarity is raised to calculate adjacency. Based on the criterion of approximate scale-free topology, we chose 14 as the soft threshold. Using the soft threshold, we calculated the adjacency (co-expression similarity) and generated a hierarchical clustering tree. The dynamic tree cut could enable the identification of modules with very similar expression profiles. The modules with highly co-expressed genes were merged. Finally, we correlated modules with external traits (herein i.e. immune score) and identified the most relevant module.

Database for Annotation, Visualization, and Integrated Discovery (DAVID) Online Tool

DAVID (version 6.8) (26) is an online bioinformatics tool that provides a comprehensive set of functional annotation tools for interpreting the biological meaning underlying specific gene sets. Herein, DAVID was used to perform the Kyoto Encyclopedia of Genes and Genomes (KEGG) pathway and Gene Ontology (GO) analysis based on the genes from the most relevant module identified using WGCNA. GO analysis can provide information on functions of genes. KEGG pathway analysis can suggest the

possible involved signaling pathways of a gene set. The brief operation process is as follows. Briefly, the symbols of the genes to be analyzed were uploaded onto the website, and *Homo sapiens* is selected as the species. Next, GO-BP-DIRECT, GO-CC-DIRECT, GO-MF-DIRECT, and KEGG PATHWAY were selected to perform functional annotation. All other parameters were set as default.

Identification and Validation of the Immune-Gene Biomarker

Overlapping genes from the most relevant module from WGCNA, immune genes from the IRIS database, and genes from GSE65904, were then analyzed using the univariate Cox regression analysis and least absolute shrinkage and selection operator (LASSO) regression analysis based on the training set I. The genes obtained from the above analysis were used for developing a prognostic immune-gene biomarker using the multivariate Cox regression analysis based on the training set I.

The prognostic signature can be quantified by calculating risk scores using multivariate Cox regression model. The predictive performance of the immune gene biomarker was assessed using area under the curve (AUC), calibration curve, Kaplan-Meier estimate in the training set I, validation set I, and test set, respectively.

Differentially Expressed Tumor-Infiltrating Immune Cell (TIICs) Analysis

TIICs between different groups were compared based on their abundance in each melanoma sample, which was calculated using CYBERSORT (**Table S2**). CYBERSORT is an *in silico* algorithm that enables the precise estimation of immune cell fractions based on RNAseq profiles of bulk samples (14). The accuracy of CYBERSORT has been demonstrated by immunohistochemistry and flow cytometry. Statistical parameters used include: p-value (t-test) and $\log_2$ fold change (logFC).

GSEA

GSEA was performed using the GSEA software (version 3.0) to detect any differences in the KEGG pathways between the low-risk and high-risk groups. The operating parameters were set as follows: the number of permutations at 1,000, weighted enrichment statistic, metric for ranking genes (Signal2Noise), max size (500), and min size (15).

Nomogram Development and Validation

To investigate the prognostic significance of the immune-gene biomarker in combination with common clinical characteristics, we planned to develop a predictive nomogram combining the immune-gene biomarker and clinical factors for melanoma patients. First, univariate Cox regression was used to screen for clinical characteristics that were significantly correlated with overall survival in the training set II. Second, clinical characteristics with a P value less than 0.05 were used to developed a nomogram using multivariate Cox regression model.

To validate the proposed nomogram, four criteria were utilized to assess prediction performance in the validation set II. First, the cases were grouped according to their predicted risk score, and Kaplan-Meier survival curves and log rank test were used to compare survival differences among the groups. Second, a concordance index (C-index) was calculated to estimate the similarity between the ranking of true survival time and of predicted risk score. The theoretical value of the C-index is between 0 and 1; a C-index larger than 0.5 indicates prediction performance better than random guessing. Third, integrated AUC was calculated. Fourth, calibration curves were plotted to evaluate the consistency between predicted survival probability and actual survival proportion at 4 years. A perfect prediction would result in a 45-degree calibration curve (i.e. the identity line).

Statistical Analyses

All statistical analysis was performed in the R Studio software (version 3.6.1). R packages "WGCNA" (13), "Vennerable" (27), "glmnet" (28, 29), "ggplot2" (30), "survival" (31), "survminer" (32), "survivalROC" (33), "rms" (34), "pROC" (35), "forestplot" (36) were used. Continuous values between the two groups were analyzed using t-tests. Non-parametric comparison between the two groups was performed using the Wilcoxon test. $P < 0.05$ was considered statistically significant.
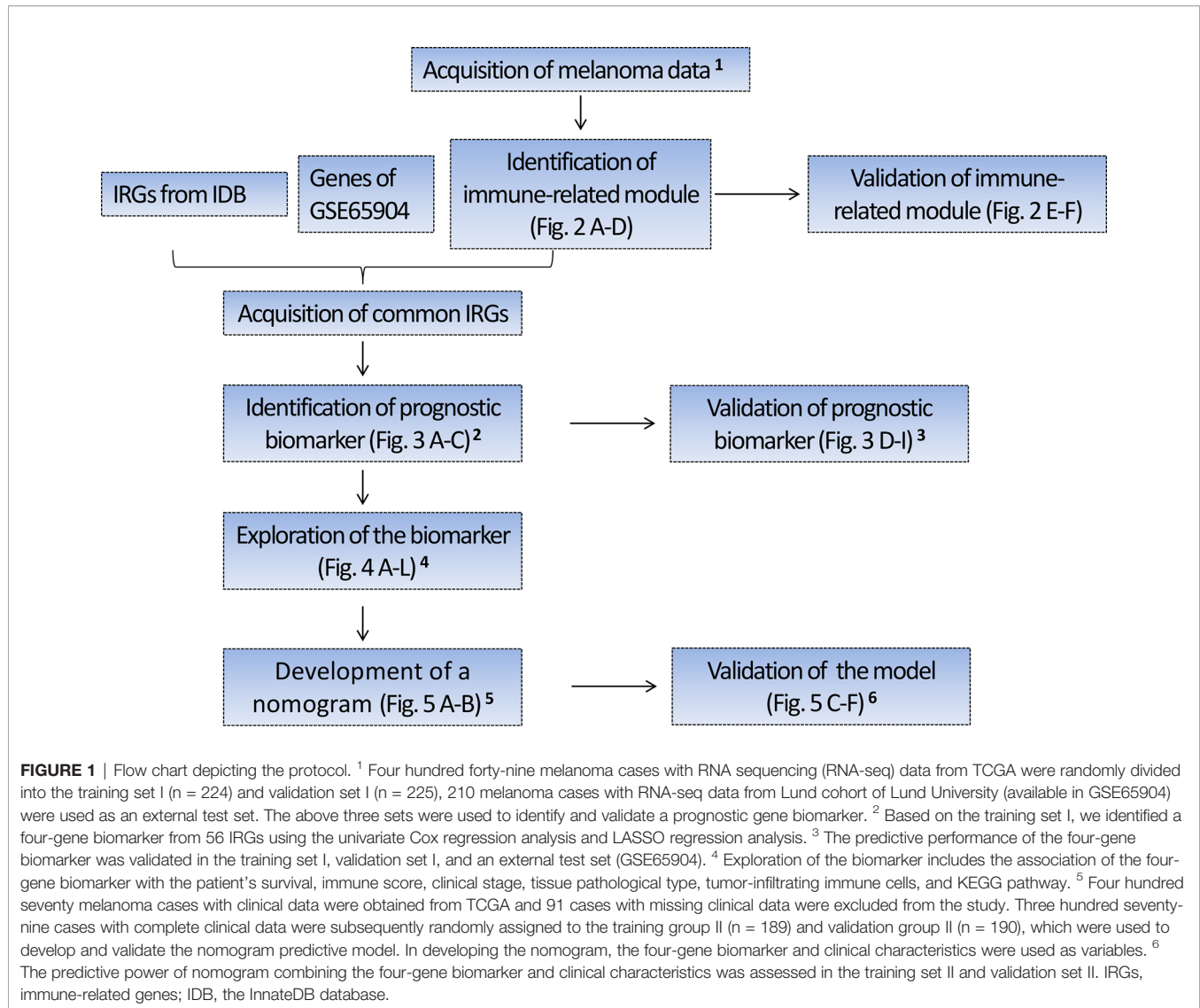
RESULTS

Study Protocol

The schematic diagram of the study protocol is shown in **Figure 1**.

Identification and Validation of the Immune-Related Module

To identify the immune-related module, the melanoma RNAseq data and the corresponding immune scores for each patient were analyzed using WGCNA. Module Black comprising 809 genes was identified as the strongest immune-related module. From 53,898 genes, we filtered out the outlier genes and genes expressed at extremely low levels to obtain 21,194 candidates for WGCNA. The soft threshold was determined as 14 (**Figures 2A, B**). All the genes were classified into 27 modules. After merging the highly co-expressed modules, 23 modules were eventually obtained (**Figure 2C**). Among them, Module Black was the strongest immune-related module (P = 3e-155, R = 0.89). Intriguingly, Module Black was also significantly associated with stromal and estimate scores in melanoma (**Figure 2D**).

To verify whether the selected module correlated with immunity, 809 genes in Module Black were analyzed using DAVID. As shown in **Figures 2 (E, F)**, the top five relevant pathways in both GO analysis and KEGG pathway were found to be immune-related.

FIGURE 1 | Flow chart depicting the protocol. [1] Four hundred forty-nine melanoma cases with RNA sequencing (RNA-seq) data from TCGA were randomly divided into the training set I (n = 224) and validation set I (n = 225), 210 melanoma cases with RNA-seq data from Lund cohort of Lund University (available in GSE65904) were used as an external test set. The above three sets were used to identify and validate a prognostic gene biomarker. [2] Based on the training set I, we identified a four-gene biomarker from 56 IRGs using the univariate Cox regression analysis and LASSO regression analysis. [3] The predictive performance of the four-gene biomarker was validated in the training set I, validation set I, and an external test set (GSE65904). [4] Exploration of the biomarker includes the association of the four-gene biomarker with the patient's survival, immune score, clinical stage, tissue pathological type, tumor-infiltrating immune cells, and KEGG pathway. [5] Four hundred seventy melanoma cases with clinical data were obtained from TCGA and 91 cases with missing clinical data were excluded from the study. Three hundred seventy-nine cases with complete clinical data were subsequently randomly assigned to the training group II (n = 189) and validation group II (n = 190), which were used to develop and validate the nomogram predictive model. In developing the nomogram, the four-gene biomarker and clinical characteristics were used as variables. [6] The predictive power of nomogram combining the four-gene biomarker and clinical characteristics was assessed in the training set II and validation set II. IRGs, immune-related genes; IDB, the InnateDB database.
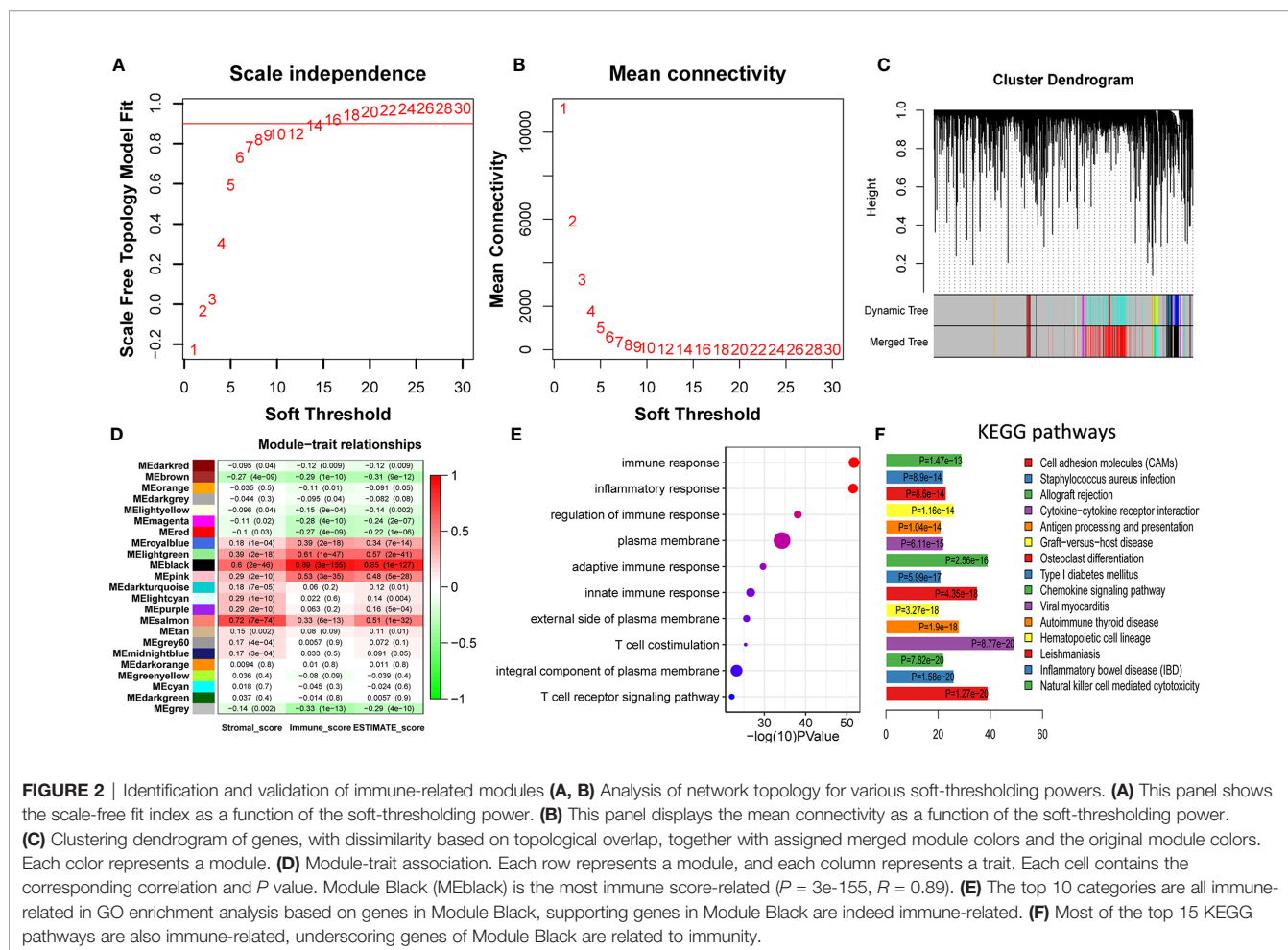
Identification and Validation of Prognostic Immune-Gene Biomarker

To select the qualified immune genes for developing an immune-gene biomarker, 56 overlapping genes were obtained by intersecting the 809 genes from Module Black (**Table S2**), 5,559 immune genes from the IRIS database, and 2,786 genes from GSE65904 (**Table S1**). First, we randomly divided 449 melanoma patients with RNA sequencing data and complete survival data from TCGA cohort into the training set I (n = 224) and validation set I (n = 225) (**Table S1**). The selected 56 genes were analyzed as variables using the univariate Cox regression analysis based on the training set I. Twelve genes with a *P* value less than 0.05 (*HLA-DQB1, CCR5, LCP2, CLEC7A, IGSF6, CLEC10A, HAPLN3, CEACAM4, IL4I1, LILRB1, FCGR1A*, and *HCP5*) were selected in the univariate Cox regression model (**Figure 3A**).

Then, the 12 genes were further screened using LASSO regression model, and four gene of *CLEC7A, CLEC10A, HAPLN3*, and *HCP5* were eventually selected to develop a four-gene biomarker using the multivariate Cox regression model (**Figures 3B, C**; detailed computational process is available in **Table S3**).

The proposed four-gene biomarker was validated in the validation set I (n = 225) and an independent testing set (GSE65904, n = 210). The 5-year AUC of the four-gene biomarker was 0.683, 0.644 and 0.645 in the training set, validation set and external test set, respectively (**Figures 3D–F**). Next, we calculated risk score of each patient using the multivariate Cox regression model based on the four-gene biomarker. The survival difference between two groups, which were grouped by the median predicted risk score, was significant (*P* value < 0.05; **Figures 3G–I**).

FIGURE 2 | Identification and validation of immune-related modules **(A, B)** Analysis of network topology for various soft-thresholding powers. **(A)** This panel shows the scale-free fit index as a function of the soft-thresholding power. **(B)** This panel displays the mean connectivity as a function of the soft-thresholding power. **(C)** Clustering dendrogram of genes, with dissimilarity based on topological overlap, together with assigned merged module colors and the original module colors. Each color represents a module. **(D)** Module-trait association. Each row represents a module, and each column represents a trait. Each cell contains the corresponding correlation and *P* value. Module Black (MEblack) is the most immune score-related (*P* = 3e-155, *R* = 0.89). **(E)** The top 10 categories are all immune-related in GO enrichment analysis based on genes in Module Black, supporting genes in Module Black are indeed immune-related. **(F)** Most of the top 15 KEGG pathways are also immune-related, underscoring genes of Module Black are related to immunity.

Relationship of Four-Gene Biomarker With Clinical Factors

Since the identified four-gene biomarker manifested prognostic relevance in patients with melanoma, we wondered if four-gene biomarker was significantly correlated with other clinical factors in melanoma. We found that risk score was negatively associated with immune score in melanoma (*P* < 0.05), indicating that the low-risk score was potentially attributed to activated immune function (**Figure 4A**). In addition, we analyzed the relationship between risk score and clinical stages, revealing that there was a significant difference in the risk score between stage I and stage II, as well as between stage II and stage III (**Figure 4B**). The four genes of *CLEC7A*, *CLEC10A*, *HAPLN3*, and *HCP5* were analyzed using log-rank tests with TCGA data, and they all showed significant survival significance (*P* < 0.05; **Figures 4E–H**), implying their protective effects on melanoma.

To explore the association between risk score and TIICs, we divided the TCGA cohort into the low-risk and high-risk groups based on the median risk score and conducted a differentially expressed TIIC analysis between these groups based on the TIIC abundance in each sample. TIIC abundance in each tissue was calculated using CYBERSORT, and the results are shown in **Supplementary Table S3**. The findings revealed that M1

macrophage, CD4$^+$ T cells, CD8$^+$ T cells, and natural killer (NK) cells were the top four upregulated TIICs in the low-risk group (**Figure 4C**), further underscoring activated immune function in this group.

Consistent with the above findings, GSEA also revealed that the top four KEGG pathways in the low-risk group were all immune-related [cytokine-cytokine receptor interaction; cell adhesion molecules (CAMs); systemic lupus erythematosus; the intestinal immune network for IgA production], while the top four pathways in the high-risk group were not immune-related (**Figures 4D, I–L**; **Table S4**).

Development and Validation of a Nomogram

Considering the prognostic significance of the four-gene biomarker, we sought to combine it with nine common clinical factors to better predict survival of melanoma patients. We first conducted a univariate Cox regression analysis to examine the prognostic significance of the four-gene biomarker and nine clinical factors, including age, gender, clinical stage, breshlow depth, clark level, tissue sample type (primary or metastatic melanoma), cancer status (with tumor or tumor-free), immune score, and new tumor event, based on the training set II. Personal
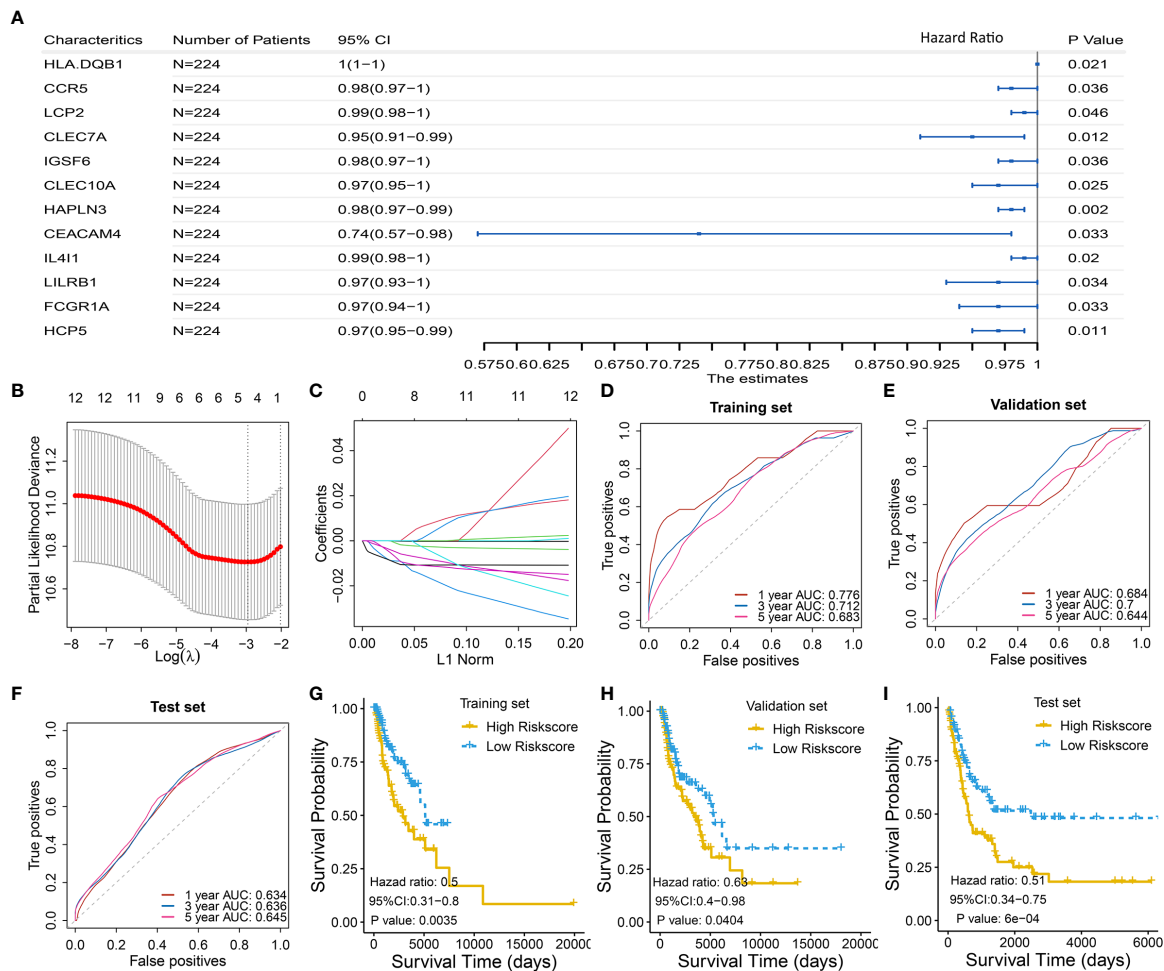
FIGURE 3 | Identification and validation of four-gene biomarker **(A)** Univariate Cox regression were used to screen for genes that were significantly correlated with overall survival in the training set I (n = 224). Twelve genes with *P* value less than 0.05 were significantly associated with overall survival, as shown in the forest plot. **(B–C)** LASSO regression was used to further eliminate redundant genes. The resulting four genes of *CLEC7A*, *CLEC10A*, *HAPLN3*, and *HCP5* were used to develop a four-gene biomarker based on multivariate Cox regression model. **(B)** Tuning parameter (λ) selection in the LASSO model used 10-fold cross-validation *via* minimum criteria. AUC was plotted *versus* log(λ). **(C)** Coefficient profiles of the fractions of 12 immune-related genes. **(D–F)** One-, 3-, and 5-year AUC were calculated for the prognostic four-gene biomarker, showing good predictive performance in the training set I, validation set I, and test set. **(G–I)** Risk scores of melanoma cases were calculated according to multivariate Cox regression model of the four genes, and grouped into low-risk and high-risk group using median risk score as threshold. Low-risk group has a significant longer survival compared to high-risk group, in the training set I, validation set I, and test set.

cancer status (with tumor/tumor-free) is one of the clinical characteristics for melanoma cases from the TCGA cohort (**Figure 5A**). Herein, we defined the personal cancer status of the tumor as cancer status. The results showed that seven factors could be used as effective prognostic characteristics for melanoma, including four-gene biomarker, immune score, age, clinical stage, cancer status, breslow depth, and clark level. Thus, the seven factors were used to developed a nomogram prognostic model based on the training set II (n = 189) (**Figure 5B**).

The proposed nomogram was assessed in the validation set II (n = 190), with a C-index of 0.736 ± 0.041 and an AUC of 0.832 ± 0.071 (**Figure 5C**). A calibration curve at 4 year (**Figure 5D**) also showed high consistency between predicted survival probability and actual survival proportion. The survival difference between

two groups, which were grouped by the median predicted risk score, was significant (*P* < 0.05; **Figures 5E, F**). The predicted risk score was calculated by adding up the score of each item using the nomogram depicted in **Figure 5B**.

DISCUSSION

We developed and validated a four-gene biomarker and a nomogram prognostic model combining a four-gene biomarker and six clinical factors for melanoma patients. The four genes (*CLEC7A*, *CLEC10A*, *HAPLN3*, and *HCP5*) were also identified as meaningful anti-tumoral genes in melanoma. Among these, *CLEC7A*, *CLEC10A*, and *HAPLN3* have not yet
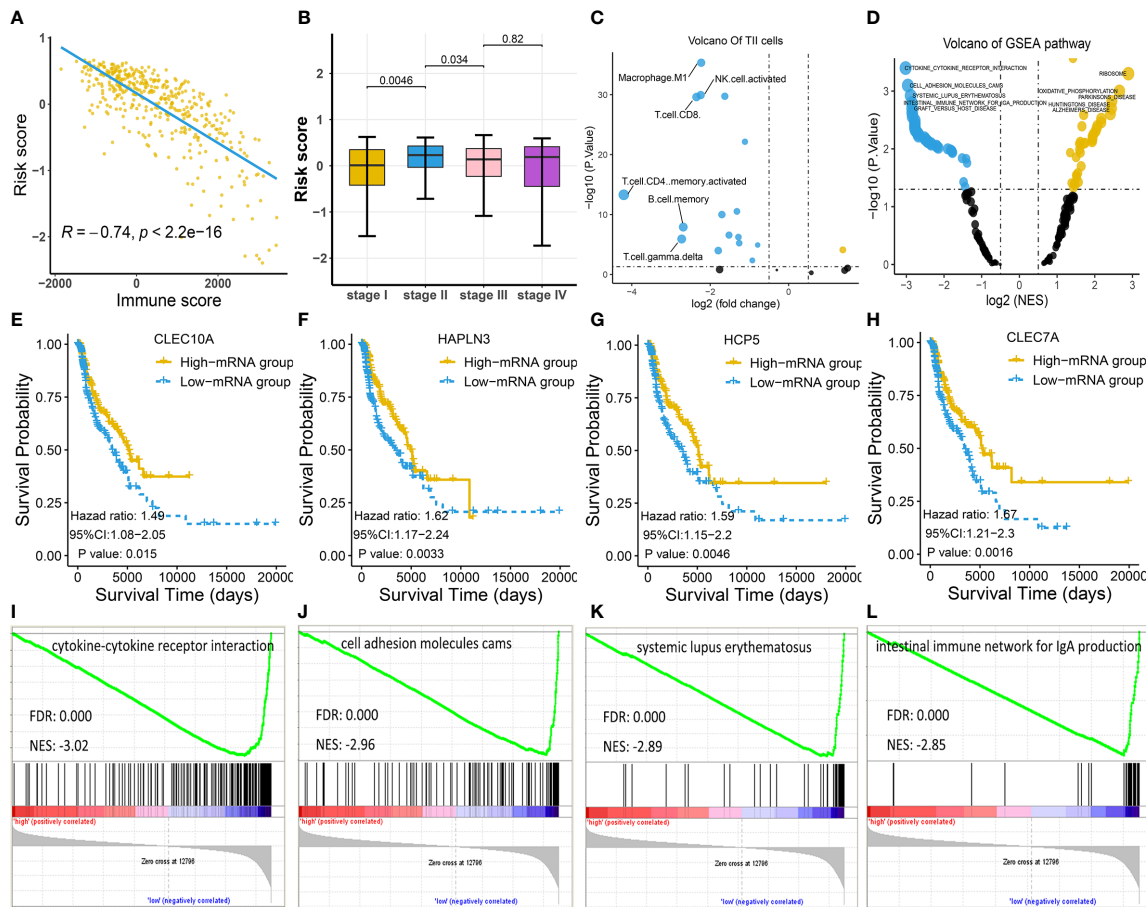
FIGURE 4 | Exploration of the four-gene biomarker **(A–C)** Risk scores of melanoma patients from TCGA cohort were calculated according to the four-gene biomarker, and the association of risk scores with common clinical characteristics were investigated. **(A)** Risk score was negatively correlated with immune score, consistent with low-risk patients who had a prolonged survival in melanoma. **(B)** There was a marked difference in risk score between stage I and stage II, as well as between stage II and stage III, implying qualitative change occurred after stage II. **(C)** The numbers of M1 macrophage, NK, CD4+, and CD8+ T cells were critically elevated in the low-risk group (the blue dot indicates TIICs whose counts are increased in the low-risk group, while the yellow dot indicates TIICs whose counts are increased in the high-risk group). **(D)** KEGG pathway analysis by GSEA displayed significantly differentially enriched pathways between the low-risk and high-risk groups. Each blue dot represents a significantly enriched pathway in the low-risk group, while yellow dot represents that in the high-risk group. **(E–H)** Four genes, CLEC7A, CLEC10A, HAPLN3, and HCP5, had a significant relevance with respect to survival; this is indicative of their anti-tumoral roles in melanoma. **(I–L)** The top four pathways in the low-risk group were all immune-related, indicating more active immune function in low-risk group compared to in the high-risk group.

been reported to be correlated with melanoma before. Furthermore, we revealed that the counts of several TIILs (M1 macrophage, NK cells, CD4+ T cells, and CD8+ T cells) were significantly elevated in the low-risk populations. In addition, the number of activated immune pathways was higher in the low-risk populations than that in the high-risk counterparts, which could provide insights for future studies. All these findings may contribute to the development of novel strategies for melanoma treatment and may provide an opportunity to perform in-depth research into the immune underpinning of melanoma.

One of the main findings of this study is the optimized immune-related prognostic biomarker comprising four immune genes (CLEC7A, CLEC10A, HAPLN3, and HCP5). The existing prognostic biomarkers usually contained at least 10 genes (37–41), a feature that would substantially reduce their clinical applicability. In contrast, the prognostic immune-related

biomarker identified herein comprises only four genes, and is therefore more convenient for clinical application. Meanwhile, the established model herein had been validated in three subsets, i.e., training, validation, and external tests, further supporting its extensive applicability.

Three genes, i.e., CLEC7A, CLEC10A, and HAPLN3 have been reported to exhibit prognostic significance with respect to melanoma for the first time, while HCP5 has been reported to inhibit the development of cutaneous melanoma (42). CLEC7A (also known as dectin-1) encodes for a pattern-recognition receptor expressed by myeloid phagocytes (macrophages, dendritic cells, and neutrophils) that can directly drive the antimicrobial activity (43, 44). Although ClEC7A activation on macrophages has been reported to induce the development of pancreatic cancer and peri-tumoral immune tolerance (45), there is no evidence regarding the relationship between CLEC7A and
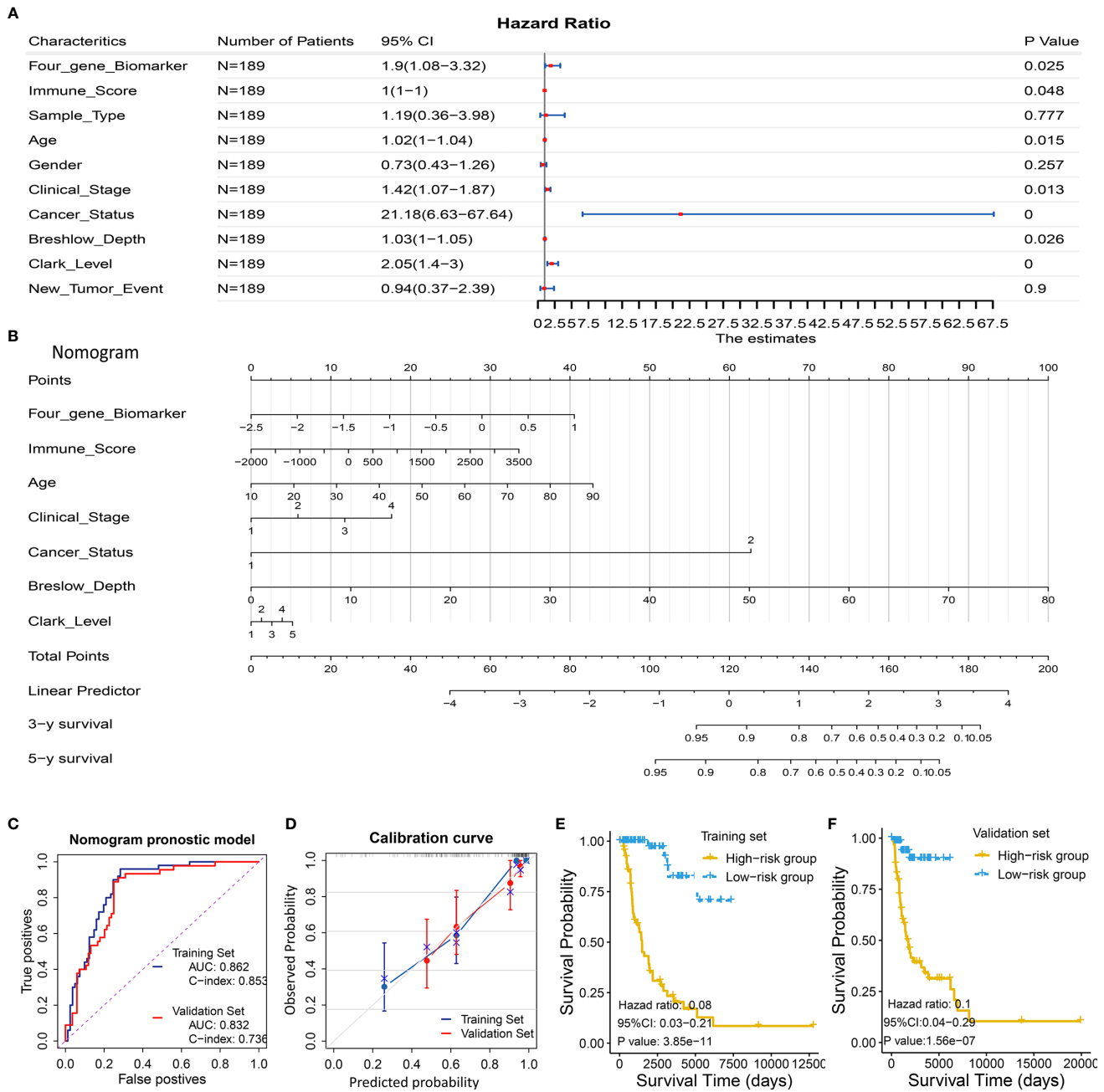
FIGURE 5 | Development and validation of a predictive nomogram for predicting survival probability. **(A, B)** Development of a predictive nomogram combing the four-gene biomarker and clinical factors in melanoma based on the training set II. **(A)** Univariate Cox regression were used to screen for clinical factors that were significantly correlated with overall survival in the training set II (n = 189), as shown in the forest plot. Seven factors including the four-gene biomarker were significantly associated with overall survival. **(B)** A nomogram combing the four-gene biomarker and clinical factors for predicting 3- and 5-year overall survival for melanoma patients. Cancer status represents personal cancer status (with tumor/tumor-free), which is one of the clinical characteristics for melanoma patients. **(C–F)** Four criteria were utilized to assess the predictive performance in the training set II and validation set II. **(C)** AUC and C-index were calculated for the nomogram prognostic models in the training set (n = 189) and validation set (n = 190). AUC of the nomogram was 0.862 ± 0.062 and 0.832 ± 0.071, and C-index was 0.853 ± 0.024 and 0.736 ± 0.041, in the training group and validation group, respectively. **(D)** Calibration curves of nomograms in training set and validation set. X-axis represents predicted probability and Y-axis represents true probability. Each point in the plot represents a subgroup of patients. Error bars represent 95% confidence intervals. 45° represents perfect prediction, and the actual performances of our nomogram are very well. **(E, F)** The resulting nomogram prognostic model was utilized to calculate risk score of cases in the training set and validation set. Low risk score subgroup had a significantly improved survival compared to high risk score (grouped according to median risk score value), in training set and validation set. The findings support the predictive power of the proposed nomogram.

melanoma. We revealed that elevated expression of *CLEC7A* could result in enhanced anti-tumoral immunity and may be correlated with prolonged survival in melanoma. *CLEC7A* could function *via* NK cells and M1 macrophages to suppress metastasis (46), consistent with the increase in the population of NK cells and M1 macrophages in the low-risk group in our study. However, the precise underlying mechanism remains largely unknown. *CLEC10A* was reported to play an important role in immune cell maturation and *CLEC10A* expression is known to correlate with improved survival in breast and ovarian cancers (47–49). Furthermore, *CLEC10A* could suppress HDM-induced Toll-like receptor 4 (TLR4)-mediated inflammatory cytokine production in mice to maintain homeostasis against inflammation. Our results demonstrate that high *CLEC10A* expression was associated with improved melanoma survival and immune scores, indicating its potential role in anti-tumoral immunity. Meanwhile, over-modulated expression of *HAPLN3* was suggested to relate with the initiation of breast cancer (50); however, its function in melanoma is presently unclear. The role of the long non-coding RNA (lncRNA) *HCP5* in cancer remains controversial. Some reports suggest that *HCP5* could induce tumor progression in cases of follicular thyroid carcinoma and lung adenocarcinoma (51–53), while others claim that *HCP5* may suppress the development of cutaneous melanoma by modulating *RARRES3* expression by sponging miR-12 (42). Consistent with previous studies, we observed an association between upregulated *HCP5* expression and improved survival in melanoma and that *HCP5* might boost the anti-tumoral immunity. Nevertheless, further *in vitro* and *in vivo* investigations are warranted to study the role of these four pivotal genes in melanoma and their precise mechanisms of action.

Our study demonstrates that the risk score was significantly associated with the immune score and tumor-infiltrating immune cell abundance, thereby supporting the importance of immune function in melanoma. M1 macrophages are associated with improved prognostic outcomes in melanoma (54–57). NK cells were confirmed to induce macrophage polarization toward the M1 phenotype and suppress tumor growth (58). Similarly, we observed higher immune scores and high abundance of M1 macrophage, CD4+, CD8+, and NK cells in the low-risk population. Further, we revealed the proportion of melanoma-infiltrating immune cells and their association with melanoma prognosis.

Another important finding is the activation of several immune pathways in the low-risk group and its correlation with prolonged survival in melanoma. Cytokine-cytokine receptor interaction pathway was the most significant in the low-risk group; this pathway plays an important role in recovery after infection with the respiratory syncytial virus as well as in colorectal cancer, renal cell carcinoma, and esophageal cancer (59–62).

This study has important implications for the treatment as well as prognosis of melanoma. First, our study provides a new prognostic biomarker and a new nomogram that could aid clinical treatment strategies for melanoma. Second, we revealed several critical immune genes, cells, and pathways that could serve as promising therapeutic targets in melanoma.

This study has a few limitations that warrant further research. First, as the four immune genes exhibit critical significance in melanoma prognoses, further *in vitro* and *in vivo* studies are required to explore their physiological mechanisms of actions. In addition, M1 macrophage, NK, CD8^{+}, and CD4^{+} T cells are indicated to benefit the survival of melanoma patients, warranting further investigation regarding the precise underlying mechanism. Third, the performance of the four-gene biomarker and similar prediction models was not statistically compared. To clarify this, we searched the PubMed database and observed that the prognostic power of the established model is still acceptable and stable as compared with that of previously established models. The 5-year AUC values of tROC for the present biomarker in training, validation, and testing sets were 0.683, 0.644, and 0.645, respectively, while those of the other models were 0.723, 0.560, and 0.682 (63); 0.648, 0.544, and 0.755 (64); and 0.68,0.65, and 0.63 (65), respectively. However, the nomogram prognostic model combing clinical factors showed a better prediction power, with an AUC value of 0.862 in the training group and 0.832 in the validation set, respectively. The drawback is that the nomogram model was not assessed in an external test set for lacking a data set with some routinely available clinical data including breslow depth, clark level, clinical stage, and survival information.

In conclusion, we successfully constructed and validated a four-gene biomarker and a nomogram prognostic model by investigating data from TCGA and GEO databases using bioinformatic tools. Our study also revealed several favorable relevant immune genes, cells, and pathways in melanoma that could serve as potential therapeutic targets. These findings provide the rationale for further investigation and would aid clinical decision-making in melanoma immunotherapy.

DATA AVAILABILITY STATEMENT

The datasets analyzed during the present study are available in the TCGA repository (https://portal.gdc.cancer.gov/) and GEO database (https://www.ncbi.nlm.nih.gov/geo/query/acc.cgi?acc=GSE65904).

ETHICS STATEMENT

Ethical review and approval were not required for the study on human participants in accordance with the local legislation and institutional requirements. The patients/participants provided their written informed consent to participate in this study. Ethical review and approval were not required for the animal study because all data are available in online database which have obtained ethical review and approval before. Written informed consent was obtained from the individual(s) for the publication

of any potentially identifiable images or data included in this article.

AUTHOR CONTRIBUTIONS

CZ and XC were responsible for the literature review and writing *Introduction* and *Discussion* of the manuscript. DD and YW analyzed the bioinformatics data and wrote *Material and Methods* and *Results* sections of the manuscript. All authors contributed to the article and approved the submitted version.

REFERENCES

1. Gershenwald JE, Guy GP Jr. Stemming the Rising Incidence of Melanoma: Calling Prevention to Action. *J Natl Cancer Inst* (2016) 108(1):djv381. doi: 10.1093/jnci/djv381
2. Tripp MK, Watson M, Balk SJ, Swetter SM, Gershenwald JE. State of the science on prevention and screening to reduce melanoma incidence and mortality: The time is now. *CA Cancer J Clin* (2016) 66:460–80. doi: 10.3322/caac.21352
3. Rastrelli M, Tropea S, Rossi CR, Alaibac M. Melanoma: epidemiology, risk factors, pathogenesis, diagnosis and classification. *In Vivo* (2014) 28:1005–11.
4. Watts CG, Madronio C, Morton RL, Goumas C, Armstrong BK, Curtin A, et al. Clinical Features Associated With Individuals at Higher Risk of Melanoma: A Population-Based Study. *JAMA Dermatol* (2017) 153:23–9. doi: 10.1001/jamadermatol.2016.3327
5. Yan Y, Leontovich AA, Gerdes MJ, Desai K, Dong J, Sood A, et al. Understanding heterogeneous tumor microenvironment in metastatic melanoma. *PloS One* (2019) 14:e0216485. doi: 10.1371/journal.pone.0216485
6. Rodríguez-Cerdeira C, Carnero Gregorio M, López-Barcenas A, Sánchez-Blanco E, Sánchez-Blanco B, Fabbrocini G, et al. Advances in Immunotherapy for Melanoma: A Comprehensive Review. *Mediators Inflamm* (2017) 2017:3264217. doi: 10.1155/2017/3264217
7. Yang S, Liu T, Nan H, Wang Y, Chen H, Zhang X, et al. Comprehensive analysis of prognostic immune-related genes in the tumor microenvironment of cutaneous melanoma. *J Cell Physiol* (2020) 235:1025–35. doi: 10.1002/jcp.29018
8. Huang R, Mao M, Lu Y, Yu Q, Liao L. A novel immune-related genes prognosis biomarker for melanoma: associated with tumor microenvironment. *Aging (Albany NY)* (2020) 12:6966–80. doi: 10.18632/aging.103054
9. Huang B, Han W, Sheng ZF, Shen GL. Identification of immune-related biomarkers associated with tumorigenesis and prognosis in cutaneous melanoma patients. *Cancer Cell Int* (2020) 20:195. doi: 10.1186/s12935-020-01271-2
10. Neagu M, Constantin C, Tanase C. Immune-related biomarkers for diagnosis/prognosis and therapy monitoring of cutaneous melanoma. *Expert Rev Mol Diagn* (2010) 10:897–919. doi: 10.1586/erm.10.81
11. Grossman RL, Heath AP, Ferretti V, Varmus HE, Lowy DR, Kibbe WA, et al. Toward a Shared Vision for Cancer Genomic Data. *N Engl J Med* (2016) 375:1109–12. doi: 10.1056/NEJMp1607591
12. Weinstein JN, Collisson EA, Mills GB, Shaw KR, Ozenberger BA, Ellrott K, et al. The Cancer Genome Atlas Pan-Cancer analysis project. *Nat Genet* (2013) 45:1113–20. doi: 10.1038/ng.2764
13. Langfelder P, Horvath S. WGCNA: an R package for weighted correlation network analysis. *BMC Bioinf* (2008) 9:559. doi: 10.1186/1471-2105-9-559
14. Newman AM, Steen CB, Liu CL, Gentles AJ, Chaudhuri AA, Scherer F, et al. Determining cell type abundance and expression from bulk tissues with digital cytometry. *Nat Biotechnol* (2019) 37:773–82. doi: 10.1038/s41587-019-0114-2
15. Subramanian A, Tamayo P, Mootha VK, Mukherjee S, Ebert BL, Gillette MA, et al. Gene set enrichment analysis: a knowledge-based approach for interpreting genome-wide expression profiles. *Proc Natl Acad Sci USA* (2005) 102:15545–50. doi: 10.1073/pnas.0506580102

16. Mootha VK, Lindgren CM, Eriksson KF, Subramanian A, Sihag S, Lehar J, et al. PGC-1alpha-responsive genes involved in oxidative phosphorylation are coordinately downregulated in human diabetes. *Nat Genet* (2003) 34:267–73. doi: 10.1038/ng1180
17. Kimball AB, Grant RA, Wang F, Osborne R, Tiesman JP. Beyond the blot: cutting edge tools for genomics, proteomics and metabolomics analyses and previous successes. *Br J Dermatol* (2012) 166(Suppl 2):1–8. doi: 10.1111/j.1365-2133.2012.10859.x
18. Shu L, Liu Y, Li J, Wu X, Li Y, Huang H. Landscape Profiling Analysis of DPP4 in Malignancies: Therapeutic Implication for Tumor Patients With Coronavirus Disease 2019. *Front Oncol* (2021) 11:624899. doi: 10.3389/fonc.2021.624899
19. Man Z, Chen Y, Gao L, Xei G, Li Q, Lu Q, et al. A Prognostic Model Based on RNA Binding Protein Predicts Clinical Outcomes in Hepatocellular Carcinoma Patients. *Front Oncol* (2020) 10:613102. doi: 10.3389/fonc.2020.613102
20. Guan X, Xu ZY, Chen R, Qin JJ, Cheng XD. Identification of an Immune Gene-Associated Prognostic Signature and Its Association With a Poor Prognosis in Gastric Cancer Patients. *Front Oncol* (2020) 10:629909. doi: 10.3389/fonc.2020.629909
21. Jung SY, Papp JC, Sobel EM, Pellegrini M, Yu H, Zhang ZF. Genetically Predicted C-Reactive Protein Associated With Postmenopausal Breast Cancer Risk: Interrelation With Estrogen and Cancer Molecular Subtypes Using Mendelian Randomization. *Front Oncol* (2020) 10:630994. doi: 10.3389/fonc.2020.630994
22. Cirenajwis H, Ekedahl H, Lauss M, Harbst K, Carneiro A, Enoksson J, et al. Molecular stratification of metastatic melanoma using gene expression profiling: Prediction of survival outcome and benefit from molecular targeted therapy. *Oncotarget* (2015) 6:12297–309. doi: 10.18632/oncotarget.3655
23. Cabrita R, Lauss M, Sanna A, Donia M, Skaarup Larsen M, Mitra S, et al. Tertiary lymphoid structures improve immunotherapy and survival in melanoma. *Nature* (2020) 577:561–5. doi: 10.1038/s41586-019-1914-8
24. Yoshihara K, Shahmoradgoli M, Martínez E, Vegesna R, Kim H, Torres-Garcia W, et al. Inferring tumour purity and stromal and immune cell admixture from expression data. *Nat Commun* (2013) 4:2612. doi: 10.1038/ncomms3612
25. Breuer K, Foroushani AK, Laird MR, Chen C, Sribnaia A, Lo R, et al. InnateDB: systems biology of innate immunity and beyond–recent updates and continuing curation. *Nucleic Acids Res* (2013) 41:D1228–33. doi: 10.1093/nar/gks1147
26. Huang da W, Sherman BT, Lempicki RA. Systematic and integrative analysis of large gene lists using DAVID bioinformatics resources. *Nat Protoc* (2009) 4:44–57. doi: 10.1038/nprot.2008.211
27. Swinton J. A package for Venn diagrams in R with the Vennerable package. (2009).
28. Friedman J, Hastie T, Tibshirani R. Regularization Paths for Generalized Linear Models via Coordinate Descent. *J Stat Softw* (2010) 33:1–22. doi: 10.18637/jss.v033.i01
29. Simon N, Friedman J, Hastie T, Tibshirani R. Regularization Paths for Cox's Proportional Hazards Model via Coordinate Descent. *J Stat Softw* (2011) 39:1–13. doi: 10.18637/jss.v039.i05

SUPPLEMENTARY MATERIAL

The Supplementary Material for this article can be found online at: https://www.frontiersin.org/articles/10.3389/fonc.2021.593587/full#supplementary-material

30. Hadley Wickham WC, Henry L, Pedersen TL, Takahashi K, Wilke C, Woo K, et al. *Dewey Dunnington, ggplot2: Elegant Graphics for Data Analysis*. New York: Springer-Verlag (2016).

31. Grambsch PM, Therneau TM. *Modeling Survival Data: Extending the Cox Model*. New York: Springer (2000).

32. Kosinski M, Kassambara A, Biecek P, Fabian S. *A Package for Drawing Survival Curves using "ggplot2" in R*. (2020).

33. Saha-Chaudhuri P, Heagerty PJ. A Package for Compute time-dependent ROC curve from censored survival data using Kaplan-Meier (KM) or Nearest Neighbor Estimation (NNE) method of Heagerty, Lumley & Pepe in R. (2013).

34. Harrell FEJr. *A Package for Regression Modeling Strategies in R*. (2020).

35. Robin X, Turck N, Hainard A, Tiberti N, Lisacek F, Sanchez JC, et al. pROC: an open-source package for R and S+ to analyze and compare ROC curves. *BMC Bioinf* (2011) 12:77. doi: 10.1186/1471-2105-12-77

36. Max Gordon TL. A Package for Advanced Forest Plot Using 'grid' Graphics in R. (2020).

37. Wu M, Li X, Zhang T, Liu Z, Zhao Y. Identification of a Nine-Gene Signature and Establishment of a Prognostic Nomogram Predicting Overall Survival of Pancreatic Cancer. *Front Oncol* (2019) 9:996. doi: 10.3389/fonc.2019.00996

38. Zhu X, Tian X, Sun T, Yu C, Cao Y, Yan T, et al. GeneExpressScore Signature: a robust prognostic and predictive classifier in gastric cancer. *Mol Oncol* (2018) 12:1871–83. doi: 10.1002/1878-0261.12351

39. Shen S, Wang G, Zhang R, Zhao Y, Yu H, Wei Y, et al. Development and validation of an immune gene-set based Prognostic signature in ovarian cancer. *EBioMedicine* (2019) 40:318–26. doi: 10.1016/j.ebiom.2018.12.054

40. Liu GM, Zeng HD, Zhang CY, Xu JW. Identification of a six-gene signature predicting overall survival for hepatocellular carcinoma. *Cancer Cell Int* (2019) 19:138. doi: 10.1186/s12935-019-0858-2

41. Zhang J, Zhang X, Piao C, Bi J, Zhang Z, Li Z, et al. A long non-coding RNA signature to improve prognostic prediction in clear cell renal cell carcinoma. *Bio Med Pharmacother* (2019) 118:109079. doi: 10.1016/j.biopha.2019.109079

42. Wei X, Gu X, Ma M, Lou C. Long noncoding RNA HCP5 suppresses skin cutaneous melanoma development by regulating RARRES3 gene expression via sponging miR-12. *Onco Targets Ther* (2019) 12:6323–35. doi: 10.2147/OTT.S195796

43. Goodridge HS, Reyes CN, Becker CA, Katsumoto TR, Ma J, Wolf AJ, et al. Activation of the innate immune receptor Dectin-1 upon formation of a 'phagocytic synapse'. *Nature* (2011) 472:471–5. doi: 10.1038/nature10071

44. Kankkunen P, Teirilä L, Rintahaka J, Alenius H, Wolff H, Matikainen S. (1,3)-beta-glucans activate both dectin-1 and NLRP3 inflammasome in human macrophages. *J Immunol* (2010) 184:6335–42. doi: 10.4049/jimmunol.0903019

45. Daley D, Mani VR, Mohan N, Akkad N, Ochi A, Heindel DW, et al. Dectin 1 activation on macrophages by galectin 9 promotes pancreatic carcinoma and peritumoral immune tolerance. *Nat Med* (2017) 23:556–67. doi: 10.1038/nm.4314

46. Mattiola I, Tomay F, De Pizzol M, Silva-Gomes R, Savino B, Gulic T, et al. The macrophage tetraspan MS4A4A enhances dectin-1-dependent NK cell-mediated resistance to metastasis. *Nat Immunol* (2019) 20:1012–22. doi: 10.1038/s41590-019-0417-y

47. Kurze AK, Buhs S, Eggert D, Oliveira-Ferrer L, Müller V, Niendorf A, et al. Immature O-glycans recognized by the macrophage glycoreceptor CLEC10A (MGL) are induced by 4-hydroxy-tamoxifen, oxidative stress and DNA-damage in breast cancer cells. *Cell Commun Signal* (2019) 17:107. doi: 10.1186/s12964-019-0420-9

48. Hoober JK, Eggink LL, Cote R. Stories From the Dendritic Cell Guardhouse. *Front Immunol* (2019) 10:2880. doi: 10.3389/fimmu.2019.02880

49. Kanemaru K, Noguchi E, Tahara-Hanaoka S, Mizuno S, Tateno H, Denda-Nagai K, et al. Clec10a regulates mite-induced dermatitis. *Sci Immunol* (2019) 4(42):eaax6908. doi: 10.1126/sciimmunol.aax6908

50. Kuo SJ, Chien SY, Lin C, Chan SE, Tsai HT, Chen DR. Significant elevation of CLDN16 and HAPLN3 gene expression in human breast cancer. *Oncol Rep* (2010) 24:759–66. doi: 10.3892/or_00000918

51. Liang L, Xu J, Wang M, Xu G, Zhang N, Wang G, et al. LncRNA HCP5 promotes follicular thyroid carcinoma progression via miRNAs sponge. *Cell Death Dis* (2018) 9:372. doi: 10.1038/s41419-018-0382-7

52. Jiang L, Wang R, Fang L, Ge X, Chen L, Zhou M, et al. HCP5 is a SMAD3-responsive long non-coding RNA that promotes lung adenocarcinoma metastasis via miR-203/SNAI axis. *Theranostics* (2019) 9:2460–74. doi: 10.7150/thno.31097

53. Kulski JK. Long Noncoding RNA HCP5, a Hybrid HLA Class I Endogenous Retroviral Gene: Structure, Expression, and Disease Associations. *Cells* (2019) 8(5):480. doi: 10.3390/cells8050480

54. Falleni M, Savi F, Tosi D, Agape E, Cerri A, Moneghini L, et al. M1 and M2 macrophages' clinicopathological significance in cutaneous melanoma. *Melanoma Res* (2017) 27:200–10. doi: 10.1097/CMR.0000000000000352

55. Cao M, Yan H, Han X, Weng L, Wei Q, Sun X, et al. Ginseng-derived nanoparticles alter macrophage polarization to inhibit melanoma growth. *J Immunother Cancer* (2019) 7:326. doi: 10.1186/s40425-019-0817-4

56. Kou Y, Ji L, Wang H, Wang W, Zheng H, Zou J, et al. Connexin 43 upregulation by dioscin inhibits melanoma progression via suppressing malignancy and inducing M1 polarization. *Int J Cancer* (2017) 141:1690–703. doi: 10.1002/ijc.30872

57. Khan Z, Cao DY, Giani JF, Bernstein EA, Veiras LC, Fuchs S, et al. Overexpression of the C-domain of angiotensin-converting enzyme reduces melanoma growth by stimulating M1 macrophage polarization. *J Biol Chem* (2019) 294:4368–80. doi: 10.1074/jbc.RA118.006275

58. Paul S, Chhatar S, Mishra A, Lal G. Natural killer T cell activation increases iNOS(+)CD206(-) M1 macrophage and controls the growth of solid tumor. *J Immunother Cancer* (2019) 7:208. doi: 10.1186/s40425-019-0697-7

59. Qian Z, Zhang Z, Wang Y. T cell receptor signaling pathway and cytokine-cytokine receptor interaction affect the rehabilitation process after respiratory syncytial virus infection. *PeerJ* (2019) 7:e7089. doi: 10.7717/peerj.7089

60. Liu J, Li H, Sun L, Wang Z, Xing C, Yuan Y. Aberrantly methylated-differentially expressed genes and pathways in colorectal cancer. *Cancer Cell Int* (2017) 17:75. doi: 10.1186/s12935-017-0444-4

61. Li F, Guo P, Dong K, Guo P, Wang H, Lv X. Identification of Key Biomarkers and Potential Molecular Mechanisms in Renal Cell Carcinoma by Bioinformatics Analysis. *J Comput Biol* (2019) 26:1278–95. doi: 10.1089/cmb.2019.0145

62. Yamamura K, Baba Y, Nakagawa S, Mima K, Miyake K, Nakamura K, et al. Human Microbiome Fusobacterium Nucleatum in Esophageal Cancer Tissue Is Associated with Prognosis. *Clin Cancer Res* (2016) 22:5574–81. doi: 10.1158/1078-0432.CCR-16-1786

63. Tian M, Yang J, Han J, He J, Liao W. A novel immune checkpoint-related seven-gene signature for predicting prognosis and immunotherapy response in melanoma. *Int Immunopharmacol* (2020) 87:106821. doi: 10.1016/j.intimp.2020.106821

64. Wan Q, Jin L, Su Y, Liu Y, Li C, Wang Z. Development and validation of autophagy-related-gene biomarker and nomogram for predicting the survival of cutaneous melanoma. *IUBMB Life* (2020) 72:1364–78. doi: 10.1002/iub.2258

65. Sheng Y, Tong L, Geyu L. An immune risk score with potential implications in prognosis and immunotherapy of metastatic melanoma. *Int Immunopharmacol* (2020) 88:106921. doi: 10.1016/j.intimp.2020.106921